ARTIFICIAL NEURAL NETWORK-BASED SPECIFIC CUTTING ENERGY MODEL FOR THE ROTARY TURNING MOLD STEEL

Trung-Thanh Nguyen[1,*], Thai-Le Minh[1], Thai-Nguyen Chung[1], Truong-An Nguyen[1], Quan-Nguyen Van[1], Huu-Toan Bui[1], Hung-Le Xuan[1], Tuan-Ngo Van[1], Luan-Le Van[1]

DOI: http://doi.org/10.57001/huih5804.2024.159

ABSTRACT

The self-propelled rotary tool turning (SPRT) process is an effective solution for machining hardened steels. In this investigation, the specific cutting energy (SCE) model was developed in terms of the inclination angle (I), depth of cut (D), feed rate (f), and spindle speed (S). A set of experiments was performed for the SKD 61 material to obtain experimental data. The Bayesian regularized feed-forward neural network was applied to develop the SCE model. The results indicated that the model's precision was acceptable due to the small deviations between the predictive and actual data. Moreover, the proposed correlation was primarily affected by the depth of cut, feed rate, spindle speed, and inclination angle, respectively. Finally, the developed SPRT operation could be utilized for machining difficult-to-cut materials.

Keywords: *Rotary turning; Specific cutting energy; Neural network; Process parameters.*

[1]Le Quy Don Technical University, Vietnam
[*]Email: trungthanhk21@mta.edu.vn
Received: 10/8/2023
Revised: 15/10/2023
Accepted: 25/5/2024

1. INTRODUCTION

Many attempts have been executed to boost performance measures for various SPRT operations. A simulation model was developed to precisely capture the machining temperature in terms of the depth of cut (D), feed rate (f), and turning speed (V) [1]. Kishawy and Wilcox emphasized that the SPRT process provided a high resistance and long tool life, while only the flank wear was produced [2]. A new flank wear model of the SPRT operation was developed, while the genetic algorithm was used to find the empirical coefficients [3]. Kishawy et al. presented that a longer tool life was obtained in rotary turning aerospace alloys, while the SR of 0.5µm was produced [4]. The artificial neural network-based models of the turning force components of the carbon steel were proposed regarding the V, D, f, and A [5]. The Oxley analysis-based model was applied to develop turning force models for the SPRT operation [6]. The results indicated that a high V decreased the friction coefficient, while the f had the highest contribution. Ezugwu presented that the turning forces and friction on the rake face of the SPRT operation were lower than the fixed ones, while a higher f decreased the surface quality [7]. Rao et al. stated that the average roughness (Ra) was decreased by 14.5% at the same material removal rate for the rotary turning of EN24 steel using the genetic algorithm [8]. Amini and Teimouri indicated that the V of 4m/min, the D of 0.3mm, and the f of 0.08mm/rev could be applied to minimize the cutting forces and Ra for the rotary turning of the AA7075 [9].

The energy consumption in the turning state (E_t), machining rate, and Ra models of the SPRT process of the hardened steel were enhanced by 50.3%, 33.2%, and 19.8%, respectively using optimal V, A, f, and D [10]. Nguyen et al. indicated that the energy efficiency was improved by 8.9% and the machining cost was decreased by 14.8% at the optimal SPRT variables [11]. However, the SCE model for the SPRT mold steel has not been developed. Moreover, the impacts of the process parameters on the SCE model have not been explored.

In this paper, we present the optimization approach and experiment setting for the SPRT process of the hardened steel. Next, the obtained results are scientifically discussed. Finally, conclusions are drawn and future research is suggested.

2. METHODS

The specific cutting energy (SCE) is defined as a ratio of the energy consumed in the SPRT process (TE) and material removal volume (MRV) and is computed as:

$$SCE = \frac{TE}{MRV} \tag{1}$$

The MRV is computed as:

$$MRV = V \times f \times D \times t_c \tag{2}$$

Where the V, f, D, and t_c are the turning speed, feed rate, depth of cut, and turning time, respectively.

The TE of the SPRT process consists of six parts, including the startup (E_s), the standby (E_{st}), transition (E_{ts}), air-turning

(E_a), turning (EC), and tool change (E_{tc}) stages. Therefore, the TE model can be expressed as:

$$TE = E_s + E_{st} + E_{ts} + E_a + EC + E_{tc} \quad (3)$$

Practically, the E_{st}, E_{ts}, E_a, and E_{tc} are constant values. In this investigation, the energy consumption in the turning stage is considered; hence, the SCE is expressed as:

$$SCE = \frac{EC}{MRV} = \frac{P_c \times t_c}{MRR \times t_c} = \frac{P_c}{MRR} \quad (4)$$

where P_c is the power consumed in the turning stage.

In the current work, the properties of the cutting insert and workpiece are considered as constants. Four key factors having the ranges, including the inclination angle, depth of cut, feed rate, and spindle speed are exhibited in Table 1. The parameter levels are identified based on the characteristics of the machine tool and the recommendations of the manufacturer of the round insert. These ranges are confirmed by the suggestions from the aforementioned works.

Table 1. Optimizing process factors.

Symbol	Parameters	Ranges
I	Inclination angle (deg.)	20-35-50
D	Turning depth (mm)	0.2-0.4-0.6
f	Feed rate (mm/rev.)	0.3-0.5-0.7
S	Spindle speed (RPM)	800-100-1200

The procedure is expressed as:

Step 1: Performing turning experiments using the Box-Behnken design [12].

Step 2: The SCE model are developed regarding process parameters by means of the BRFFNN approach [13].

For the BRFFNN, the weights of the network are random variables. The probability density function is expressed as:

$$P = \frac{P(D|w,\beta,M)P(w|\alpha,M)}{P(D|\alpha,\beta,M)} \quad (5)$$

where D and M present the obtained data and the forward multi-layer perceptron, respectively. w and P(w|α,M) are the vector and prior knowledge of network weights, respectively. When the Gaussian function is employed, the likehood-P (D|w, β, M) is expressed as:

$$P(D|w,\beta,M) = \frac{1}{\left(\frac{\pi}{\beta}\right)^{n/2}} e^{-\beta d_d} \quad (6)$$

where d_d is the sum of squared deviations for data.

The normalized factor P (D|α, β, M) is expressed as:

$$P(D|w,\beta,M) = \frac{1}{\left(\frac{\pi}{\alpha}\right)^{N/2}} e^{-\alpha d_W} \quad (7)$$

where d_w is the sum of squared errors for the weights.

The probability density function is expressed as:

$$P = \frac{1}{Z_F(\alpha,\beta)} e^{-(\beta d_d + \alpha d_W)} \quad (8)$$

The numerical experiments of each BRFFNN model are executed to calculate the mean square error (MSE), which is expressed as:

$$MSE = \frac{1}{N}\sum_{i=1}^{N}(y_a - y_P)^2 \quad (9)$$

where y_a and y_p are the actual and predictive values, respectively. N denotes the number of testing points. The best BRFFNN architecture is chosen with the lowest MSE value.

Step 3: Evaluation of the accuracy of the SCE model at random points.

3. EXPERIMENTAL SETTING

The round bar with the mold material entitled SKD61 steel is employed as the turning workpiece. The external diameter and length of each specimen are 40mm and 320mm, respectively. The hardened steel having a hardness of 56 HRC is selected because of the applications in the fabrication of mold pins.

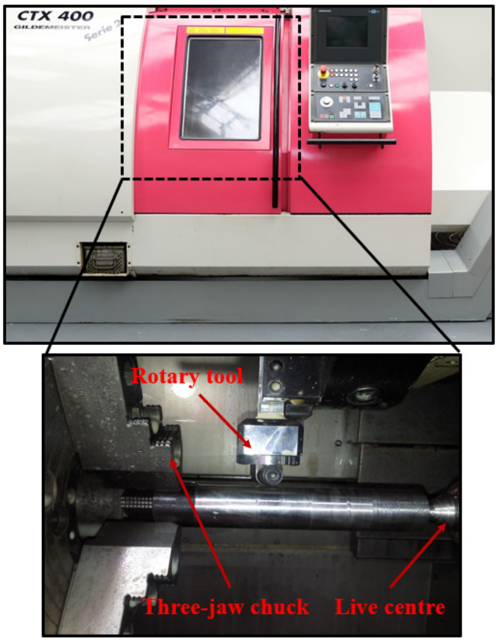

Fig. 1. Experimental setting for the rotary turning process

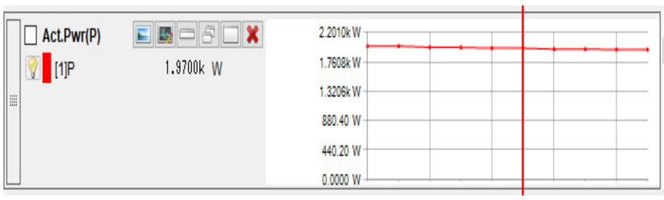

Fig. 2. Turning power at experimental No. 19

The experiments are executed with the support of a CNC lathe entitled GILDEMEISTER CTX 400 Serie 2 (Fig. 1). A power meter labeled KEW6305 is employed to capture power components during the rotary turning. An interval of

0.1 sec. is used to improve the accuracy of the measured data. The example results of the turning experiments are shown in Fig. 2.

4. RESULTS AND DISCUSSIONS

4.1. Development of *SCE* model

Table 2 presents the experimental outcomes. The operating parameters of the BRFFNN model, including the NH, PF, TF, NL, and LF are shown in Table 3. The computational trials of the BRFFNN are performed based on the parameter combination entitled Taguchi L_{18}. As a result, the optimal data of the HN, PM, TF, HL, and LF are 24, MSEREG, logsig, 3, and LearnGDM, respectively (Fig. 3).

To confirm the precision of the developed ANN model, the comparisons between the experimental and predictive results are conducted. Table 4 indicates the comparative values at different points. As a result, the computed deviations of the *SCE* from lies from -0.73% to 0.74%. The small errors revealed that the proposed model ensure the prediction accuracy.

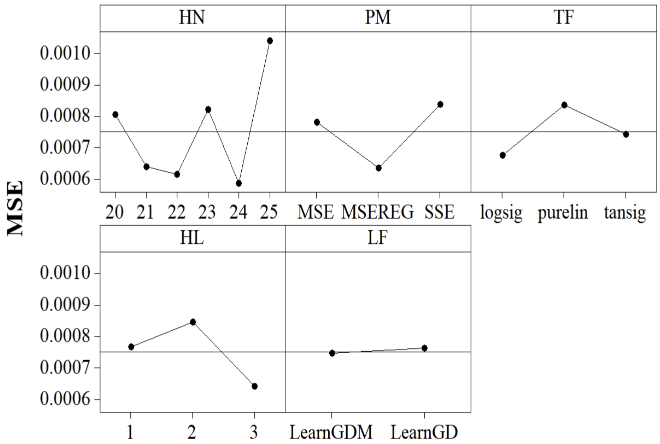

Fig. 3. The MSE values with different operating parameters

Table 2. Experimental data of the rotary turning

No.	I (deg.)	D (mm)	f (mm/rev.)	S (rpm)	SCE (J/mm³)
Experimental data for developing *SCE* model					
1	20	0.4	0.5	1200	4.31
2	35	0.6	0.5	800	3.76
3	50	0.4	0.3	1000	7.54
4	20	0.6	0.5	1000	3.27
5	35	0.6	0.5	1200	2.92
6	35	0.6	0.7	1000	2.38
7	20	0.4	0.3	1000	7.09
8	35	0.2	0.5	800	9.58
9	35	0.4	0.3	800	7.81
10	50	0.6	0.5	1000	3.42
11	20	0.2	0.5	1000	8.84
12	35	0.4	0.7	800	4.12
13	50	0.4	0.5	800	5.71
14	35	0.4	0.5	1000	4.52
15	35	0.4	0.7	1200	3.12
16	20	0.4	0.5	800	5.47
17	35	0.2	0.7	1000	6.33
18	20	0.4	0.7	1000	3.63
19	35	0.6	0.3	1000	4.81
20	35	0.4	0.3	1200	6.56
21	35	0.2	0.5	1200	7.78
22	35	0.4	0.5	1000	4.53
23	50	0.2	0.5	1000	9.11
24	50	0.4	0.7	1000	3.77
25	50	0.4	0.5	1200	4.49
26	35	0.2	0.3	1000	12.31
Experimental data for testing SCE model					
27	25	0.3	0.4	900	8.02
28	30	0.5	0.6	1100	2.73
29	40	0.3	0.5	1050	6.15
30	45	0.6	0.7	1200	2.71
31	50	0.3	0.6	950	8.15
32	40	0.5	0.4	1200	4.12

Table 3. Operating parameters of the BRNN model

Symbol	Operating inputs	Ranges
NH	Number of hidden neurons	20; 21; 22; 23; 24; 25
PF	Performance function	MSE; MSEREG; SSE
TF	Transfer function	Logsig; Purelin; Tansig
NL	Number of hidden layers	1; 2; 3
LF	Learning function	LearnGDM; LearnGD

Table 4. Confirmations of the precision of the developed models

No.	SCE (J/mm³)		
	Experiment	Prediction	Errors
27	8.02	8.04	-0.25
28	2.73	2.71	0.73
29	6.15	6.12	0.49
30	2.71	2.69	0.74
31	8.15	8.12	0.37
32	4.12	4.15	-0.73

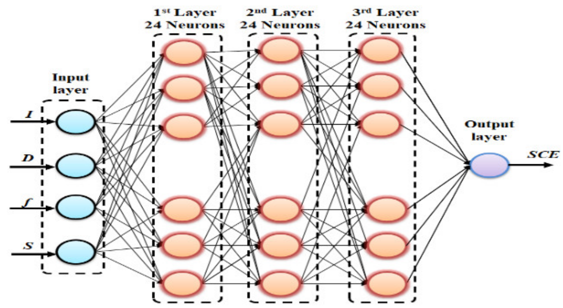

Fig. 4. The structure of the BFRNN model

4.2. ANOVA results

The ANOVA results of the SCE are shown in Table 5. Significant parameters are single factors (I, D, f, and S), interactive factors (Df and DS), and quadratic factors (I^2, D^2, f^2, and S^2). The contributions of the I, D, f, and S are 1.31%, 30.35%, 20.73%, and 6.63%, respectively. The contributions of the Df and DS are 9.68% and 2.66%, respectively. The contributions of the I^2, D^2, f^2, and S^2 are 3.39%, 14.13%, 7.26%, and 13.2%, respectively. The values of the R^2 value (0.9784), the adjusted R^2 (0.9684), and the predicted R^2 (0.9562) indicate that the SCE model is adequate.

Table 5. ANOVA results for the SCE model.

Source	Sum of Squares	Mean Square	F-value	p-value	Remark	Contribution (%)
Model	149.4020	10.6716	31.1539	< 0.0001	Significant	
I	20.6606	20.6606	60.3229	0.0286	Significant	1.31
D	478.6637	478.6637	1397.5583	< 0.0001	Significant	30.35
f	326.9423	326.9423	954.5761	< 0.0001	Significant	20.73
S	104.5648	104.5648	305.2986	< 0.0001	Significant	6.63
ID	4.8892	4.8892	14.2749	0.7597	Insignificant	0.31
If	13.5635	13.5635	39.6013	0.404	Insignificant	0.86
IV	1.4194	1.4194	4.1443	0.873	Insignificant	0.09
Df	152.6677	152.6677	445.7451	< 0.0001	Significant	9.68
DS	41.9521	41.9521	122.4878	0.0162	Significant	2.66
fS	9.9360	9.9360	29.0103	0.5076	Insignificant	0.63
I^2	53.4652	53.4652	156.1029	0.0072	Significant	3.39
D^2	222.8507	222.8507	650.6589	< 0.0001	Significant	14.13
f^2	114.5008	114.5008	334.3088	< 0.0001	Significant	7.26
S^2	31.0698	31.0698	90.7147	0.0348	Significant	1.97
Residual	3.7680	0.3425				
Total	153.17					
$R^2 = 0.9754$; Adj. $R^2 = 0.9684$; Pred. $R^2 = 0.9562$						

4.3. Parametric influences

As shown in Fig. 5a, a higher inclined angle decreases the contact area between the insert and the workpiece; hence, the material volume to be cut decreases. The material is softly removed and the SCE decreases. A further angle increases the contact area due to the perpendicular direction between the cutting tool and workpiece; hence, the material volume to be cut increases. The material is hardly turned; hence, the SCE increases.

As shown in Fig. 5b, a higher D increases the contact area between the insert and workpiece; hence, a higher thickness of the chip is produced. The material is hardly processed; hence, the energy consumption increases. Dortunately, the SCE is inversely proportional to the increase in the D; hence, the SCE decreases.

As shown in Fig. 5c, a higher f increases the distance between the successive turning paths; hence, the turning time decreases. The SCE consequently decreases with an increased f.

As shown in Fig. 5d, a higher S increases the machining temperature at the turning region, leading to reductions in the hardness and strength of the workpiece. The material is easily removed; hence, low SCE consumes.

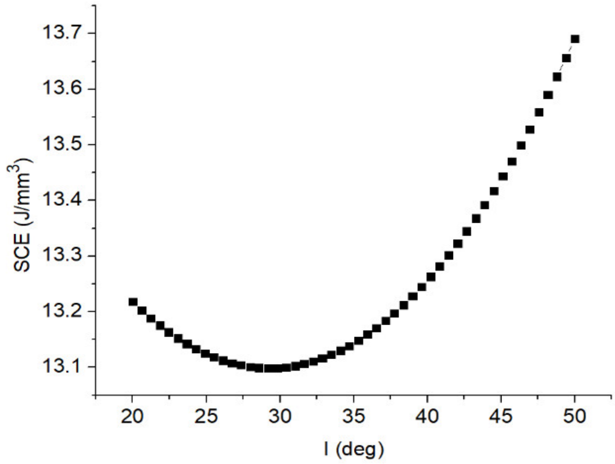

(a) SCE versus I

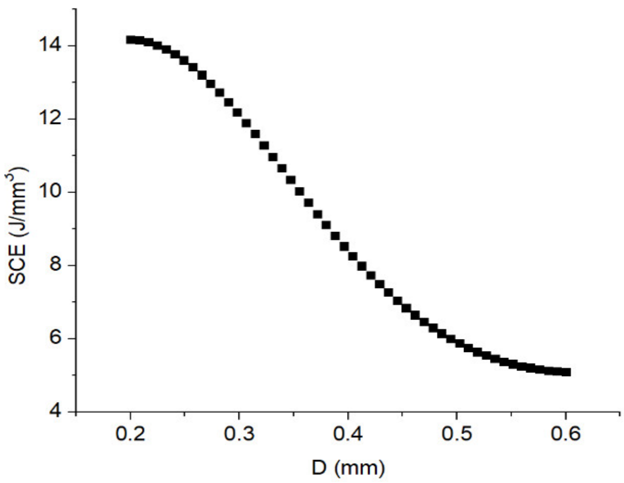

(b) SCE versus D

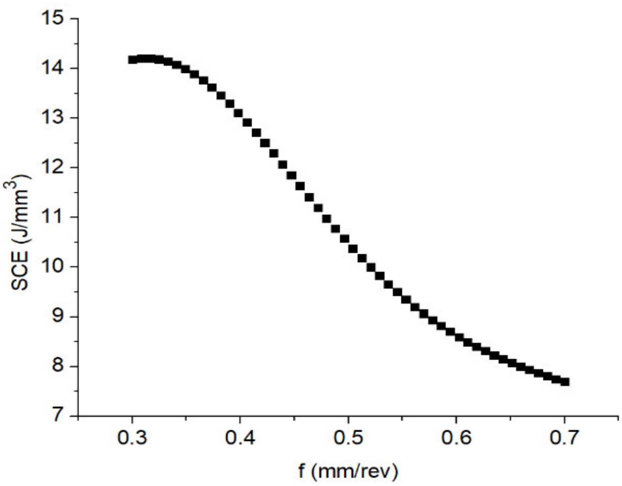

(c) SCE versus f

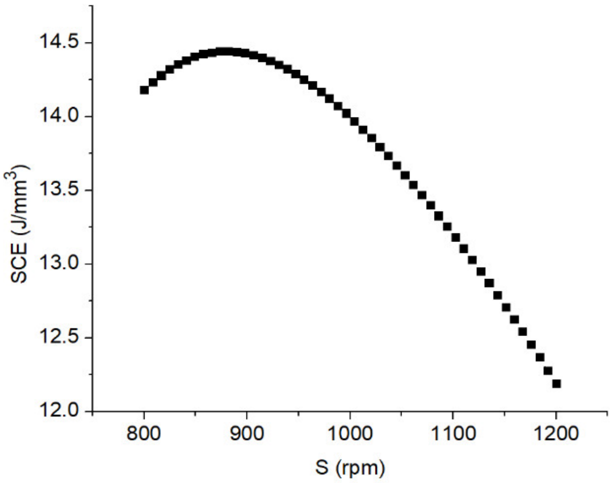

(d) SCE versus S

Fig. 5. The impacts of process parameters on the SCE

5. CONCLUSIONS

In this investigation, the specific cutting energy (SCE) model of the SPRT process were decreased using optimal factors, including the inclination angle (I), depth of cut (D), feed rate (f), and spindle speed (S). The BRFFNN-assisted models were applied to construct the SCE. The conclusions can be expressed as:

1. For the SCE model, the depth of cut was named as the most effective parameter, followed by the feed rate, spindle speed, and inclination angle, respectively.

2. For minimizing the SCE, the middle value of the I could be applied, while low D, f, and S were recommended.

3. The proposed SCE model could be applied to predict the response value in the rotary turning.

4. The impacts of SPRT factors on air pollution and carbon emissions have been not analyzed. A holistic optimization will be performed to address more environmental metrics.

REFERENCES

[1]. Dessoly V., Melkote S.N., Lescalier C., "Modeling and verification of cutting tool temperatures in rotary tool turning of hardened steel," *Int. J. Mach. Tools Manuf.*, 44, 1463-1470, 2004.

[2]. Kishawy H.A., Wilcox J., "Tool wear and chip formation during hard turning with self-propelled rotary tools," *Int. J. Mach. Tools Manuf.*, 43, 433-439, 2003.

[3]. Kishawy H.A., Pang L., Balazinski M., "Modeling of tool wear during hard turning with self-propelled rotary tools," *Int. J. Mech. Sci.*, 53, 1015-1021, 2011.

[4]. Kishawy H.A., Becze C.E., McIntosh D.G., "Tool performance and attainable surface quality during the machining of aerospace alloys using self-propelled rotary tools," *J. Mater. Process. Technol.*, 152, 266-271, 2004.

[5]. Wang S.H., Zhu X., Li X., Turyagyenda G., "Prediction of cutting force for self-propelled rotary tool using artificial neural networks," *J. Mater. Process. Technol.*, 180, 23-29, 2006.

[6]. Li L., Kishawy H.A., "A Model for cutting forces generated during machining with self-propelled rotary tools," *Int. J. Mach. Tools. Manuf.,* 46, 1388-1394, 2006.

[7]. Ezugwu E.O., "Improvements in The Machining of Aero-Engine Alloys using Self-Propelled Rotary Tooling Technique," *J. Mater. Process. Technol.*, 185, 60-71, 2007.

[8]. Rao T.B., Krishna A.G., Katta R.K., Krishna K.R., "Modeling and multi-response optimization of machining performance while turning hardened steel with self-propelled rotary tool," *Adv. Manuf.*, 3, 84-95, 2015.

[9]. Amini S., Teimouri R., "Parametric study and multicharacteristic optimization of rotary turning process assisted by longitudinal ultrasonic vibration," *Proc. Inst. Mech. Eng. E: J. Process Mech. Eng.,* 231(5), 978-991, 2017.

[10]. Nguyen T.T., "An Energy-efficient optimization of the hard turning using rotary tool," *Neural Comput. & Applic.,* 33, 2621-2644, 2020.

[11]. Nguyen T.T., Duong Q.D., Mia M., "Sustainability-based optimization of the rotary turning of the hardened steel," *Metals*, 10, 939, 2020.

[12]. Trung D.D., "Application of TOPSIS an PIV methods for multi - criteria decision making in hard turning process," *Journal of Machine Engineering*, 21(4), 57-71, 2021.

[13]. Nguyen A., Nguyen V., Le T., Nguyen N., "A Hybridization of machine learning and NSGA-II for multi-objective optimization of surface roughness and cutting force in ANSI 4340 alloy steel turning," *Journal of Machine Engineering*, 23(1), 133-153, 2023.